ACS Macro Letters

Letter

pubs.acs.org/macroletters

Cavitation in Block Copolymer Modified Epoxy Revealed by In Situ Small-Angle X-Ray Scattering

Carmelo Declet-Perez, Lorraine F. Francis, and Frank S. Bates*

Department of Chemical Engineering and Materials Science, University of Minnesota, Minneapolis, Minnesota 55455, United States

Supporting Information

ABSTRACT: Simultaneous small-angle X-ray scattering (SAXS) and tensile experiments were performed on epoxies modified with approximately 30 nm diameter rubbery and glassy core block copolymer micelles. The in situ SAXS data, interpreted using established analytical models, reveals efficient and coherent cavitation of the spherical rubbery cores coincident with yielding and absence of cavitation in the glassy nanodomains. These results are quantitatively anticipated by recent theory that accounts for cavitation in rubber toughened plastics as a function of particle size.

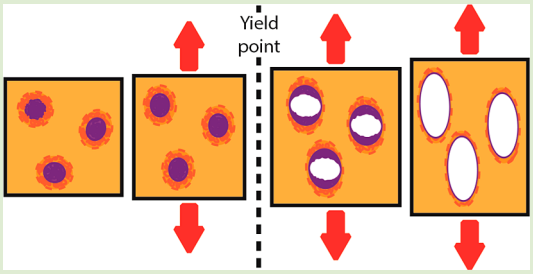

Addition of rubber particles to epoxy thermoset plastics has been a successful approach for toughening these inherently brittle materials.[1] Despite the effectiveness of this strategy, a complete description of the toughening mechanism, particularly for submicrometer-sized particles, is still elusive. Moreover, relatively high concentrations of added rubber are required to achieve the desired toughness, which can reduce the stiffness (elastic modulus) and use temperature (glass transition temperature) of the product. Internal cavitation of well-bonded rubber particles is acknowledged to occur during deformation of rubber-modified epoxies; however, its relevance and consequences in toughening mechanisms remain controversial.[2−5] Our group is particularly interested in understanding the enhanced toughness achieved upon adding small amounts of block copolymers[6−8] to epoxy resins, a technology recently commercialized by The Dow Chemical Company under the trade name Fortegra.

Using an energy balance approach, critical cavitation conditions were initially developed by Gent and co-workers for bulk rubbers by considering the growth of preexisting flaws.[9,10] Subsequently, Lazzeri and Bucknall adapted the cavitation criteria in addressing how rubber particles respond to triaxial strains when embedded in a glassy matrix.[3] They showed that the critical volumetric strain required to induce cavitation increases monotonically with decreasing particle size. More recently, Bucknall and Paul[11,12] have extended these concepts to account for the energy released from the matrix upon cavitation and the effect of interacting voids, both aspects being generally applicable to rubber toughened plastics.

This letter describes small-angle X-ray scattering (SAXS) experiments performed in situ while simultaneously stretching a model thermoset epoxy modified with poly(styrene-*b*-ethylene oxide) (PS-PEO) and poly(ethylene-*alt*-propylene-*b*-ethylene oxide) (PEP-PEO) to give glassy and rubbery core block copolymer micelles, respectively. The experimental results provide insight into the local deformation processes leading to enhanced toughness in this class of commercially important materials. Recent work from our group demonstrated evidence of cavitation in 15 nm diameter block copolymers micelles in epoxies based on TEM observations of subcritical cracks.[7] Owing to the restricted field of view afforded by TEM and due to the complex nature of the process zone ahead of a propagating crack, it was difficult to assess the extent of particle cavitation in this region. To overcome this limitation, we devised the experiments reported here. Our findings regarding cavitation in relatively low concentrations of 30 nm diameter rubbery domains (5% by weight block copolymer which translates to about 4% by volume micelle cores) embedded in the epoxy matrix are quantitatively anticipated by the theory of Bucknall and Paul.[11,12]

SAXS patterns were recorded while simultaneously straining specimens in tension. Similar methods have been applied to rubber-modified thermoplastics,[13−15] semicrystalline polymers,[16−18] and filled elastomers.[19−21] Figure 1 shows the modified tensile bar specimen used for the in situ experiments along with representative load−displacement curves for the neat and modified epoxies. The nontraditional geometry of the in situ specimens does not allow for rigorous calculations of the tensile properties of our materials. Nonetheless, the linear elastic modulus E is proportional to the slope of the load versus displacement curve at small displacements, which equals 700 ± 140, 710 ± 5, and 590 ± 60 N/mm for the neat epoxy and epoxies modified with PS-PEO and PEP-PEO, respectively. These results agree with previous measurements[7,22] that show little change in E when 5% by weight PEP-PEO is added to various thermoset epoxies. Nominal yield stresses for the in situ measurements, 77 ± 6, 77.7 ± 0.3 and 68.4 ± 0.6 MPa for the neat, and PS-PEO and PEP-PEO modified specimens,

Received: August 24, 2013
Accepted: October 1, 2013
Published: October 4, 2013

   dx.doi.org/10.1021/mz4004419 | *ACS Macro Lett.* 2013, 2, 939−943

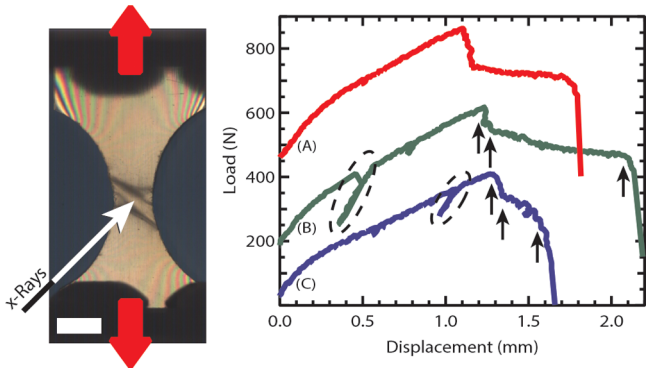

Figure 1. (Left) Modified bar under tension showing neck growth. The X-ray beam passes through the narrow portion of the bar where the plastic deformation is localized. Scale bar equals 3 mm. (Right) Representative load vs displacement curves for (A) neat epoxy and epoxies modified with (B) glassy and (C) rubbery core micelles. Curves A and B were shifted vertically for clarity by 400 and 150 N, respectively. Arrows in curves B and C denote the following stages of deformation for which scattering patterns are provided below: just prior to the yield point, just after the yield point, and prior to failure. Dotted ellipses identify artifacts in the curves.[23]

respectively, were calculated using the initial cross-sectional area at the narrowest point of the specimens (i.e., closest distance between the semicircular stress concentrators). Displacements at break were determined to be 2.0 ± 0.6 mm (neat epoxy), 2.1 ± 0.2 mm (PS-PEO), and 1.8 ± 0.3 mm (PEP-PEO). These property values represent the average (±range) of three (neat and PEP-PEO) and two (PS-PEO) measurements. Separate tensile experiments on the neat material using a standard dog bone geometry confirmed the magnitude (within experimental error) and discontinuous nature of the yield point.

Representative 2D SAXS patterns obtained from the block copolymer modified epoxies at different stages of deformation are illustrated in Figure 2. Up to the yield point (identified as the maximum load in the load−displacement curves in Figure 1) both the PS-PEO and PEP-PEO modified materials produced scattering patterns with circular features consistent with randomly dispersed spherical micelles. Clear differences develop beyond the yield point. A dramatic increase in intensity, accompanied by the development of distinct anisotropy, is evident in the SAXS patterns obtained from the rubbery core modified epoxy. In contrast, the glassy core-based specimen produced almost no change in the scattered intensity upon yielding. Further elongation leads to noticeably greater anisotropy with PEP-PEO, and the evolution of an elliptical scattering pattern with PS-PEO, followed by fracture. Here we restrict our attention to the central portions of the 2-D SAXS patterns, which derive from intra- and interparticle interference; a more complete assessment of these results will be presented elsewhere.

The small-angle scattering intensity from randomly dispersed axisymmetric micelles can be described by the following relationship:[24]

$$I(q) = n_p \times \Delta\bar{\rho}^2 \times \langle F^2(\mathbf{q})\rangle \times S'(q) \quad (1)$$

where $q = |\mathbf{q}| = 4\pi\lambda^{-1}\sin(\theta/2)$ is the magnitude of the scattering vector, n_p is the number of particles, $\Delta\bar{\rho}$ is the

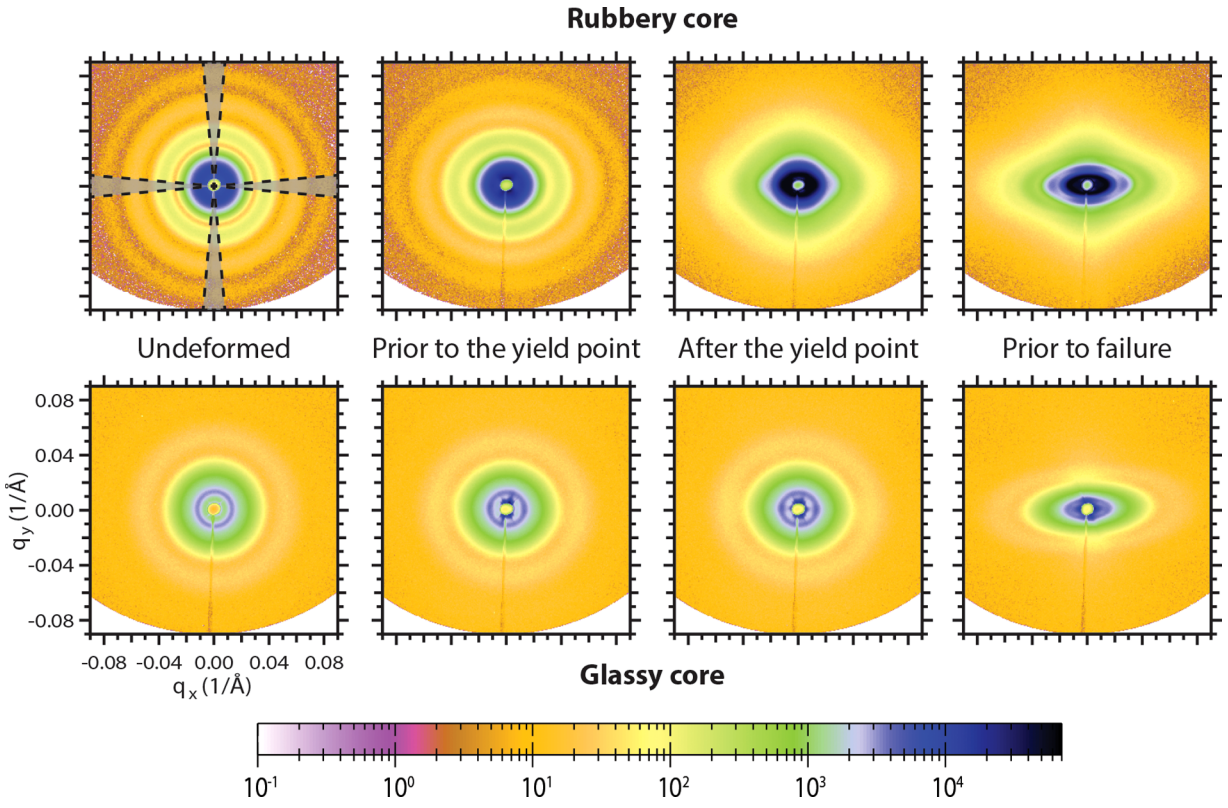

Figure 2. 2D SAXS patterns at different stages of deformation for epoxies modified with rubbery (top row) and glassy (bottom row) core micelles. Tensile load applied along vertical direction. First panel on top row shows 10° sectors parallel and perpendicular to the tensile direction used for azimuthal integrations. Intensity scale in arbitrary units. Same q scale used for all patterns.

dx.doi.org/10.1021/mz4004419 | ACS Macro Lett. 2013, 2, 939−943

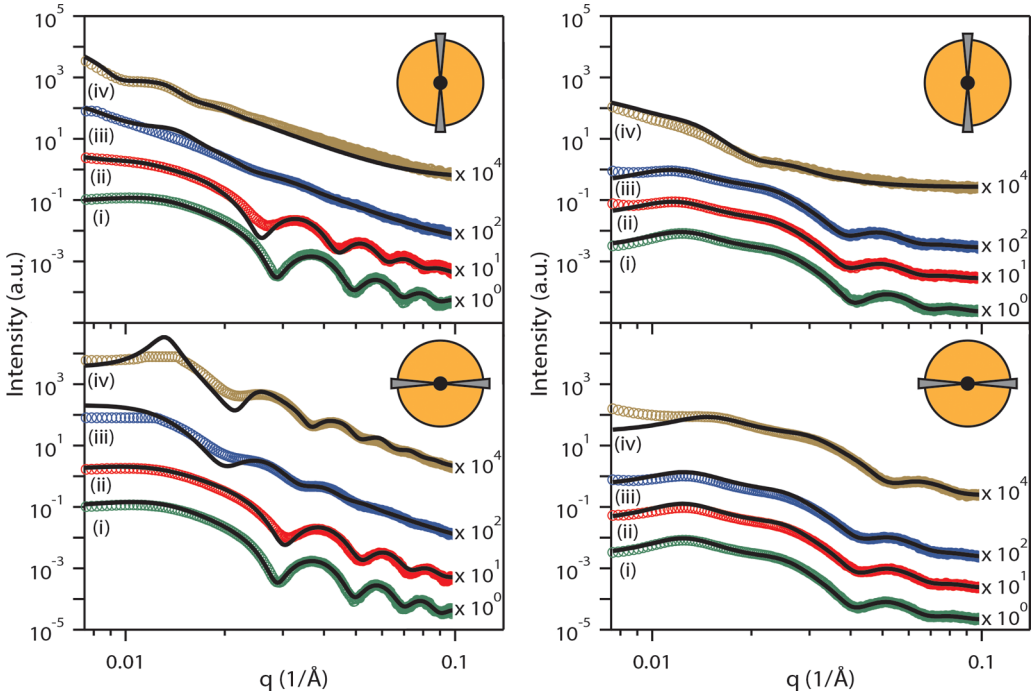

Figure 3. 1D integrations of scattering patterns for rubbery (left) and glassy (right) core micelles in the directions parallel and perpendicular to the tensile load as indicated by the insets. Curves correspond to different stages of deformation: (i) undeformed, (ii) just prior to the yield point, (iii) right after the yield point, and (iv) just prior to failure. Scattering data was modeled according to eq 1. Curves were shifted vertically for clarity.

difference in electron density (i.e., SAXS contrast), $F(\mathbf{q})$ is the amplitude of the scattered waves, $S'(q)$ is the structure factor for an ensemble of particles with a distribution of sizes, and $\langle ... \rangle$ denotes an average taken with respect to the size of the particles (see Supporting Information for details). In our model, the PEO corona and epoxy matrix are assumed to be contrast-matched; consequently, we only consider scattering from the micelle cores. Figure 3 shows the experimental intensities for rubbery and glassy core micelles integrated across sectors along two orthogonal directions at different stages of deformation. The associated fits to these data using eq 1, assuming uniform arrays of elliptically shaped cores, are shown by the solid curves. Despite its simplicity, this model describes the data quite well, particularly in the q ranges dominated by intraparticle correlations, the focus of this publication.[25] Two characteristic dimensions (minor and major axes of the ellipse) are extracted from these fits from which the core volume V has been calculated.

Figure 4 illustrates how the normalized volume (V/V_0) changes with reduced sample displacement (l/l_y), where V_0 and l_y are the undeformed core volume and displacement at the yield point, respectively. The rubbery and glassy core modified epoxies respond very differently to large strain deformation. Prior to the yield point both types of micelles maintain a constant volume. After the yield point, the glassy cores deform at constant volume until failure. In sharp contrast, the volume of the rubbery cores roughly doubles upon yielding and continues to dilate with further extension, reaching approximately five times the initial value prior to failure.

These results provide important insights regarding the microscopic events that occur during loading of block copolymer modified epoxies. The formation of a neck in the region outlined by the semicircular stress concentrators generates a local state of triaxial stress, analogous to that found in a standard tensile specimen geometry.[26] Therefore,

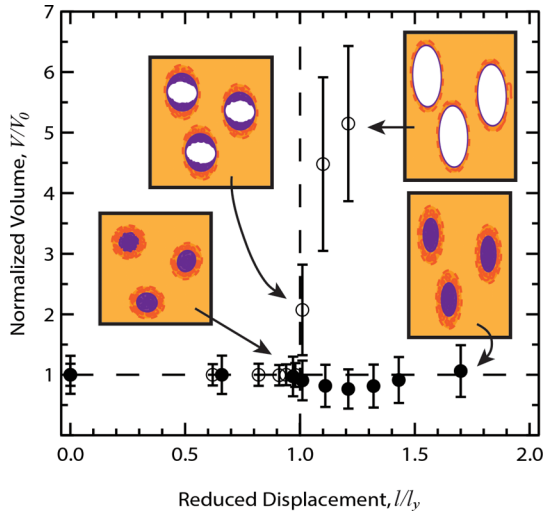

Figure 4. Change in volume as a function of deformation for rubbery (open circles) and glassy (filled circles) core micelles. Volume calculated assuming micelle shapes change from spherical to ellipsoidal (prolate) as deformation proceeds. Vertical dashed line denotes the yield point. Horizontal dashed line denotes constant volume. Schematic representation of selected stages of deformation are included. Error bars calculated by propagation of error analysis of the volume calculation using the mean and standard deviation of the core dimensions extracted from the model.

the stress state in the material in this zone, which is illuminated by the X-ray beam, mimics that found ahead of a propagating crack in fracture experiments and actual applications. Coincident with the yield point, the PEP-PEO micelles cavitate, either within the rubbery core or through debonding at the PEO/epoxy interface. Absence of cavitation in the PS-PEO nanocomposites, which have the same micelle corona structure

dx.doi.org/10.1021/mz4004419 | ACS Macro Lett. 2013, 2, 939−943

as PEP-PEO, strongly implicates cavitation within the rubbery cores, as depicted in the illustrations included with Figure 4. This mode of failure also is consistent with the large jump in overall scattering intensity that accompanies yielding. Based on the model fits the intensity increases by approximately 15 times. Within about 15% this intensity gain is accounted for by the increase in contrast factor ($\Delta\overline{\rho}^2$) that results from the creation of a void (with scattering length density $\overline{\rho}_{void} = 0$) in every micelle, that is, consistent with the simultaneous cavitation of all the rubbery cores; representative calculations are provided in the Supporting Information.

Recently, Bucknall and Paul,[11,12] building on earlier work by Lazerri and Bucknall,[3] extended the theoretical model accounting for a size-dependent cavitation criterion and included the role of particle concentration in rubber toughening of plastics. Here we summarize the predictions of this model based on material parameters relevant to the PEP-PEO modified epoxy reported in this letter; see the Supporting Information for the relevant calculations. A full assessment of the theory will be presented in a separate publication. Three regimes are anticipated by the theory for a 4% by volume concentration of rubber particles: (1) no cavitation in particles with a diameter below 23 nm; (2) cavitation coincident with yielding in particles between 23 and 70 nm in diameter; (3) cavitation prior to yielding in particles larger than 70 nm. Our results are consistent with mechanism 2. For the 30 nm diameter rubber particles described here, a critical uniaxial tensile stress of 122 MPa is predicted to induce simultaneous yielding and cavitation (see Supporting Information). This prediction is roughly 80% greater than the measured yield stress of 68 MPa. However, this calculated critical stress does not account for static stress within the rubber particles, which develops when the nanocomposite is cooled below the glass transition temperature of the matrix. It is well-known that the mismatch in thermal expansion coefficient between glassy (α_g) and rubbery (α_r) polymers, $\alpha_r \cong 3\alpha_g$, leads to a significant hydrostatic tension in the rubber,[27,28] which lowers the macroscopic applied stress required to cavitate the embedded particles. We have estimated a hydrostatic tension within the rubbery PEP cores at room temperature of about 33 MPa due to this effect (see Supporting Information), reducing the predicted macroscopic applied tensile stress required for cavitation to 89 MPa, which, within experimental error is consistent with our result. (Note that the in situ tensile geometry does not precisely satisfy the plain strain condition assumed in the calculation. Also, there is some ambiguity in assigning the effective rubber particle radius due to the role played by the corona region; see below).

Following cavitation the voids continue to expand with further extension of the specimen (see Figure 4) in response to the increasing local hydrostatic tension. Assuming that the total number of micelles remains constant during deformation and neglecting changes in specimen thickness, cavitation and subsequent void growth increases the volume fraction of the rubbery micelle cores from an initial value of 0.04 to approximately 0.24 (i.e., about 20% of the sample volume is occupied by voids just prior to failure). Guild et al. have estimated volume changes upon cavitation of micrometer size rubber particles in epoxy using finite element techniques.[29] These calculations considerably underestimate the particle expansion reported here. We suspect that the nanoscale dimension of the block copolymer micelles is responsible for this disagreement. Larger particles require larger scale displacement of the cross-linked network than smaller ones at a constant overall volume of expansion of the rubber, that is, the consequences of particle dilation are not scale invariant. This also implies that more tightly cross-linked materials (i.e., smaller molecular weight between cross-links) will be less susceptible to cavitation induced toughening, which is supported by our previous work.[8,22] As the micelles dilate the local network must plastically deform, a mechanism that both absorbs energy by strain hardening and likely facilitates shear yielding. Guild et al.[29] also predicted that cavitation accelerates the growth of shear bands in response to a state of triaxial stress, which relates to the events that occur ahead of a crack tip.

Finally, we emphasize that rubber cavitation alone does not account for enhanced toughness in all block copolymer modified epoxies. As demonstrated in our preliminary report,[30] glassy core forming PS-PEO micelles, which do not cavitate as shown here, produce half the toughness as the PEP-PEO additive in the limit of high molecular weights between cross-links. (Here we note that the area under the curves in Figure 1 should not be interpreted as a direct measure of toughness for comparison with compact tension fracture measurements, i.e., G_{1c}.[30] Cavitation leads to a porous material and the associated tensile failure mechanisms do not reflect the events that occur around the tip of a propagating crack.) This observation unambiguously implicates the PEO-rich corona region surrounding each micelle. We conclude that rubber cavitation serves as a trigger that amplifies the effects of PEO-based corona disruption,[30] promoting massive plastic deformation of the matrix in the form of void growth and shear bands.

EXPERIMENTAL SECTION

Two types of block copolymer were synthesized following well-established protocols, poly(styrene-*b*-ethylene oxide) (M_n = 56.5 kg/mol, w_{PEO} = 0.53, M_n/M_w = 1.10) and poly(ethylene-*alt*-propylene-*b*-ethylene oxide) (M_n = 13.6 kg/mol, w_{PEO} = 0.36, M_n/M_w = 1.10), where M_n and M_w are the number and weight average molecular weights, respectively, and w_{PEO} is the weight fraction of PEO. Both block copolymers form relatively monodisperse spherical micelles in cured epoxy containing glassy (PS) and rubbery (PEP) cores (see Supporting Information). The thermoset plastic matrix, described in detail elsewhere,[8] is based on a combination of epoxy (diglycidyl ether of bisphenol A marketed as D.E.R. 332 by The Dow Chemical Company) and a mixture of di- and trifunctional phenolic curing agents [bisphenol A (Dow Chemical) and 1,1,1-tris(4-hydroxyphenyl) ethane (Aldrich)]. A theoretical molecular weight between cross-links of 3000 g/mol was targeted for all formulations. Neat and block copolymer modified (5 wt %) epoxy plaques were prepared as detailed in an earlier publication.[30] Fully cured plaques were machined into modified tensile bars containing two semicircular stress concentrators that position plastic deformation at a specific location in the specimen (Figures 1 and S2).

In situ SAXS allowed us to follow real-time changes in the block copolymer nanostructure upon straining the specimens. The experiments were conducted at the Argonne National Laboratory using beamline 5-ID-D with 17 keV radiation (wavelength λ = 0.729 Å) and a sample-to-detector distance of 4.58 m. The narrow portion of the specimen was centered along the path of the ~18 μm diameter beam. A dual-actuator hydraulic Instron machine (Model AW3601-1) kept the same area of the specimen exposed to the X-ray beam at all times until failure. All specimens were strained at room temperature with a constant cross-head speed of 0.5 mm/min. SAXS patterns were simultaneously collected every 5 s until failure using a Mar 165 mm CCD detector.

dx.doi.org/10.1021/mz4004419 | ACS Macro Lett. 2013, 2, 939−943

■ ASSOCIATED CONTENT

Supporting Information

TEM images of block copolymer micelles in epoxy, dimensions of modified tensile bar for in situ SAXS experiments, description of scattering model and fitting parameters, parameters used for calculation of contrast change upon cavitation, parameters used for calculation of thermal stresses, and parameters used for calculation of stress map for block copolymer modified epoxies. This material is available free of charge via the Internet at http://pubs.acs.org.

■ AUTHOR INFORMATION

Corresponding Author

*E-mail: bates001@umn.edu.

Notes

The authors declare no competing financial interest.

■ ACKNOWLEDGMENTS

This work was supported by the National Science Foundation through the University of Minnesota MRSEC under Award Number DMR-0819885. We thank Prof. William Gerberich, Dr. Feng Zuo, Dr. Brian Habersberger, and Grayce Theryo for helpful discussions. The epoxy resin and bisphenol A were provided by The Dow Chemical Company. Portions of this work were performed at the DuPont-Northwestern-Dow Collaborative Access Team (DND-CAT) located at Sector 5 of the Advanced Photon Source (APS). DND-CAT is supported by E.I. DuPont de Nemours and Co., The Dow Chemical Company, and Northwestern University. Use of the APS, an Office of Science User Facility operated for the U.S. Department of Energy (DOE) Office of Science by Argonne National Laboratory, was supported by the U.S. DOE under Contract No. DE-AC02-06CH11357.

■ REFERENCES

(1) Bagheri, R.; Marouf, B. T.; Pearson, R. A. *Polym. Rev.* **2009**, *49*, 201−225.

(2) Pearson, R. A.; Yee, A. F. *J. Mater. Sci.* **1991**, *26*, 3828−3844.

(3) Lazzeri, A.; Bucknall, C. B. *J. Mater. Sci.* **1993**, *28*, 6799−6808.

(4) Huang, Y.; Kinloch, A. J. *J. Mater. Sci. Lett.* **1992**, *11*, 484−487.

(5) Huang, Y.; Kinloch, A. J. *J. Mater. Sci.* **1992**, *27*, 2753−2762.

(6) Dean, J. M.; Lipic, P. M.; Grubbs, R. B.; Cook, R. F.; Bates, F. S. *J. Polym. Sci., Part B: Polym. Phys.* **2001**, *39*, 2996−3010.

(7) Liu, J. (D.); Sue, H.-J.; Thompson, Z. J.; Bates, F. S.; Dettloff, M.; Jacob, G.; Verghese, N.; Pham, H. *Macromolecules* **2008**, *41*, 7616−7624.

(8) Thompson, Z. J.; Hillmyer, M. A.; Liu, J. (D.); Sue, H.-J.; Dettloff, M.; Bates, F. S. *Macromolecules* **2009**, *42*, 2333−2335.

(9) Gent, A. N.; Lindley, P. B. *Proc. R. Soc. London, Ser. A* **1959**, *249*, 195−205.

(10) Gent, A. N.; Tompkins, D. A. *J. Appl. Phys.* **1969**, *40*, 2520−2525.

(11) Bucknall, C. B.; Paul, D. R. *Polymer* **2009**, *50*, 5539−5548.

(12) Bucknall, C. B.; Paul, D. R. *Polymer* **2013**, *54*, 320−329.

(13) Bubeck, R. A.; D., J. B., Jr; Kramer, E. J.; Brown, H. R. *J. Mater. Sci.* **1991**, *26*, 6249−6259.

(14) He, C.; Donald, A. M.; Butler, M. F. *Macromolecules* **1998**, *31*, 158−164.

(15) Jansen, B. J. P.; Rastogi, S.; Meijer, H. E. H.; Lemstra, P. J. *Macromolecules* **2001**, *34*, 4007−4018.

(16) Butler, M. F.; Donald, A. M.; Ryan, A. J. *Polymer* **1998**, *39*, 39−52.

(17) Schneider, K.; Trabelsi, S.; Zafeiropoulos, N. e.; Davies, R.; Riekel, C.; Stamm, M. *Macromol. Symp.* **2006**, *236*, 241−248.

(18) Humbert, S.; Lame, O.; Chenal, J. M.; Rochas, C.; Vigier, G. *Macromolecules* **2010**, *43*, 7212−7221.

(19) Ehrburger-Dolle, F.; Hindermann-Bischoff, M.; Livet, F.; Bley, F.; Rochas, C.; Geissler, E. *Langmuir* **2001**, *17*, 329−334.

(20) Belina, G.; Urban, V.; Straube, E.; Pyckhout-Hintzen, W.; Klüppel, M.; Heinrich, G. *Macromol. Symp.* **2003**, *200*, 121−128.

(21) Zhang, H.; Scholz, A. K.; de Crevoisier, J.; Vion-Loisel, F.; Besnard, G.; Hexemer, A.; Brown, H. R.; Kramer, E. J.; Creton, C. *Macromolecules* **2012**, *45*, 1529−1543.

(22) Liu, J. (Daniel); Sue, H.-J.; Thompson, Z. J.; Bates, F. S.; Dettloff, M.; Jacob, G.; Verghese, N.; Pham, H. *Polymer* **2009**, *50*, 4683−4689.

(23) The features enclosed by the dashed lines correspond to artifacts due to the Instron control loop. These features are not discussed any further as they do not represent any real change in the specimen.

(24) Kotlarchyk, M.; Chen, S.-H. *J. Chem. Phys.* **1983**, *79*, 2461.

(25) Larger discrepancies in the low q region at deformations past the yield point arise due to a lack of a better model to describe interparticle correlations of highly anisotropic particles. See Supporting Information for details. In addition, in the case of the rubbery core micelle, cavitation results in detector saturation, despite beam attenuation.

(26) Bridgman, P. W. *Trans. Am. Soc. Met.* **1944**, *32*, 553−574.

(27) Bates, F. S.; Cohen, R. E.; Argon, A. S. *Macromolecules* **1983**, *16*, 1108−1114.

(28) Boyce, M. E.; Argon, A. S.; Parks, D. M. *Polymer* **1987**, *28*, 1680−1694.

(29) Guild, F. J.; Kinloch, A. J.; Taylor, A. C. *J. Mater. Sci.* **2010**, *45*, 3882−3894.

(30) Declet-Perez, C.; Redline, E. M.; Francis, L. F.; Bates, F. S. *ACS Macro Lett.* **2012**, *1*, 338−342.